Hindawi
Geofluids
Volume 2020, Article ID 1628431, 13 pages
https://doi.org/10.1155/2020/1628431

Research Article

Study on Fracture Morphological Characteristics of Refracturing for Longmaxi Shale Formation

Yintong Guo, Lei Wang, Xin Chang, Jun Zhou, and Xiaoyu Zhang

State Key Laboratory of Geomechanics and Geotechnical Engineering, Institute of Rock and Soil Mechanics, Chinese Academy of Sciences, Wuhan 430071, China

Correspondence should be addressed to Yintong Guo; ytguo@whrsm.ac.cn

Received 22 August 2019; Revised 17 January 2020; Accepted 6 February 2020; Published 4 March 2020

Academic Editor: Julien Bourdet

Refracturing technology has become an important means for the regeneration of old wells reconstruction. It is of great significance to understand the formation mechanism of hydraulic fracturing fracture for the design of hydraulic fracturing. In order to accurately evaluate and improve fracturing volume after refracturing, it is necessary to understand the mechanism of refracturing fracture in shale formation. In this paper, a true triaxial refracturing test method was established. A series of large-scale true triaxial fracturing experiments were carried out to characterize the refracturing fracture initiation and propagation. The results show that for shale reservoirs with weak bedding planes and natural fractures, hydraulic fracturing can not only form the main fracturing fracture, which is perpendicular to horizontal minimum principal stress, but it can also open weak bedding plane or natural fractures. The characteristics of fracturing pump curve indicated that the evolution of fracturing fractures, including initiation and propagation and communication of multiple fractures. The violent fluctuation of fracturing pump pressure curve indicates that the sample has undergone multiple fracturing fractures. The result of refracturing shows that initial fracturing fracture channels can be effectively closed by temporary plugging. The refracturing breakdown pressure is generally slightly higher than that of initial fracturing. After temporary plugging, under the influence of stress induced by the initial fracturing fracture, the propagation path of the refracturing fracture is deviated. When the new fracturing fracture communicates with the initial fracturing fracture, the original fracturing fracture can continue to expand and extend, increasing the range of the fracturing modifications. The refracturing test results was shown that for shale reservoir with simple initial fracturing fractures, the complexity fracturing fracture can be increased by refracturing after temporary plugging initial fractures. The effect of refracturing is not obvious for the reservoir with complex initial fracturing fractures. This research results can provide a reliable basis for optimizing refracturing design in shale gas reservoir.

1. Introduction

In recent years, hydraulic fracturing technology has been widely used in tight oil and gas reservoir development. The typical production characteristics of shale gas wells is that the output declines greatly and the rate is fast, which is quite different from conventional oil and gas wells. With the production of shale gas fracturing wells, the fractures formed by initial fracturing will be gradually close and become ineffective; the production of oil and gas wells will be decline. In addition, many of the early fracture treatments failed to deliver the expected results, including poor treatment practices, fracturing techniques, and poor awareness [1]. Horizontal well refracturing technology is one of the main technologies for the effective development of shale gas reservoir. Thousands of shale gas wells in North America are being refractured; as a whole, refracturing can significantly increase shale oil and gas well production and ultimately recoverable resources. At present, the mechanism of refracturing is generally understood in the following three aspects [2]: (1) reopen existing fracturing cracks; (2) effectively extend the original fracture system; (3) new fractures are opened in the initial unfractured zone. In the past decade, shale gas has been industrialized in Fuling area, Sichuan basin of China. The first shale gas wells have entered the stage where refracturing is needed to increase production. At

present, researches on physical test and theoretical analysis for fracturing fracture propagation of shale reservoir are focused on initial fracturing. Various studies have been conducted to reveal fracture morphology characteristics of shale reservoir under different conditions. It was found that with high horizontal stress difference, low-viscosity fluid can activate discontinuities to form a complex fracture network, and high-viscosity fluid is likely to produce large fractures [3]. The bedding direction of the shale plays an important role in gas fracturing [4]. True triaxial hydraulic fracturing experiment was carried out in order to understand the fracture initiation and vertical propagation behavior [5]. The influences of multiple factors (bedding planes, injection rate, in situ stress, fracturing fluid viscosity, etc.) on fracture propagation pattern were studied based on a series of hydraulic fracturing experiments. The hydraulic fracture propagation rule in random naturally fractured blocks was investigated. It is found that hydraulic fracture propagation along the natural fracture system with low horizontal stress difference coefficient is forming a single hydraulic fracture and not connecting with the natural fracture [6]. Based on the displacement discontinuity method (DDM), a two-dimensional numerical model has been developed and used to investigate the interaction between hydraulic and pre-existing natural fractures. Research has shown that the cemented strength of the NF has an important influence on the interaction mechanism [7]. In the fracturing experiment, the anisotropy of shale plays an important role in the mechanical behavior and fracture propagation. Considering anisotropy, SC-CO2 fracturing effect under different injection rate and stress state was carried out [8]. It is found that higher injection rate can lead to higher breakdown pressure, while higher deviator stress can lead to the lower breakdown pressure instead. It is estimated that the prefracture cyclic injection can reduce the rock breakdown pressure and increase the possibility of failure. Compared with conventional hydraulic fracturing, the reduction of breakdown pressure and the increase of damage during cyclic injection are quantitatively analyzed [9].

There are few studies on refracturing test. The initiation and propagation of refracturing fractures need further study. With the development of fracturing technology, some scholars have begun to pay attention to issues related to refracturing. The properties of refracturing and the conditions limiting the application of refracturing are discussed [10]. The identification method of candidate wells is introduced, and the treatment design, diagnosis technology, and economic evaluation are discussed. A new method for calculating the distribution of multicluster coal slurry has been applied in fracturing and refracturing [11]. The main advantages of this approach include (1) simple implementation; (2) no numerical evaluation of the Jacobian matrix; (3) computationally efficiency; (4) easy integration of slurry distribution, proppant transport, stress shadow effects, and multiple fracture propagation. Using a fully coupled geo-mechanical model and microseismic analysis, the effects of seismic isolation and near-wellbore friction on the refracture treatment of a typical Eagle Ford well were studied. The results show that the stress change caused by depletion can enhance the conductivity of the fracture, and the fluid distribution between the depleted zone and the undepleted zone will change during the treatment. Different hydraulic fracturing and refracturing treatments processes were proposed [12, 13]. Considering the interference from the initial fracturing fractures, a new semianalytical model is proposed to characterize the transient flow behavior of a reoriented refracture [14]. The fully coupled gas flows and stress changes of hydraulic fracturing and refracturing tight gas reservoirs are simulated by a numerical model. The results show that the anisotropy of horizontal permeability is a key parameter in the overall design of hydraulic fracturing [15]. The effects of isolation and near-wellbore friction on refracturing treatment in typical Eagle Ford Wells were studied by using a method of fully coupled geo-mechanical modeling and microseismic analysis. The case studies show that the stress changes induced by depletion can enhance stress transfer, and fluid distribution between fractures in depleted and nondepleted zones can also change [16]. Considering the parameters of volume fracturing horizontal wells, an idealized concept of refracturing well is proposed. The refracturing potential of candidate wells needs to be graded and optimized, and a numerical simulation method was used to establish a production prediction model of refracturing considering stress sensitivity [17]. The transient flow model of hydraulic fracture after refracturing is established and the orthogonality of new and old hydraulic fractures is evaluated. The model shows that the orthogonal fractures generated during the refracturing process will result in orthogonal linear flow in the simulated volume of the reservoir [18]. The viscous zone model (CZM) was established based on extended finite element method (XFEM) to simulate the process of plugging and flow diversion. The model has been verified by test results [19]. Numerical simulation method seems to be useful for identifying the refracturing fracture propagation. However, the results of these methods were inaccurate, because the calculation assumes limited height fracture propagation and ignores the interaction between the fractures and discontinuities.

Therefore, it is necessary to study the mechanism of refracturing fracture propagation in shale formations to estimate the effect of refracturing. Laboratory physical tests are effective because of the initiation and propagation of refracturing fractures can be clearly observed. In this study, the physical test method of true triaxial refracturing is established. Then, a series of true triaxial refracturing experiments were conducted to determine the mechanism of refracturing fracture propagation for Longmaxi shale formation. The effect of initial fracturing fracture on initiation and propagation of refracturing fractures was investigated. The refracturing fracture characteristics of shale samples with different initial fracturing fractures are analyzed. The research results can be helpful to further study the interaction mechanism between refracturing fractures and initial fracturing fractures.

2. Experimental Materials and Procedure

2.1. Sample Preparation. The shale samples were obtained from the outcrops of Longmaxi formation in Sichuan Basin of China. Blocks of shale were collected from the exposed rock-mass section, as shown in Figure 1. The average

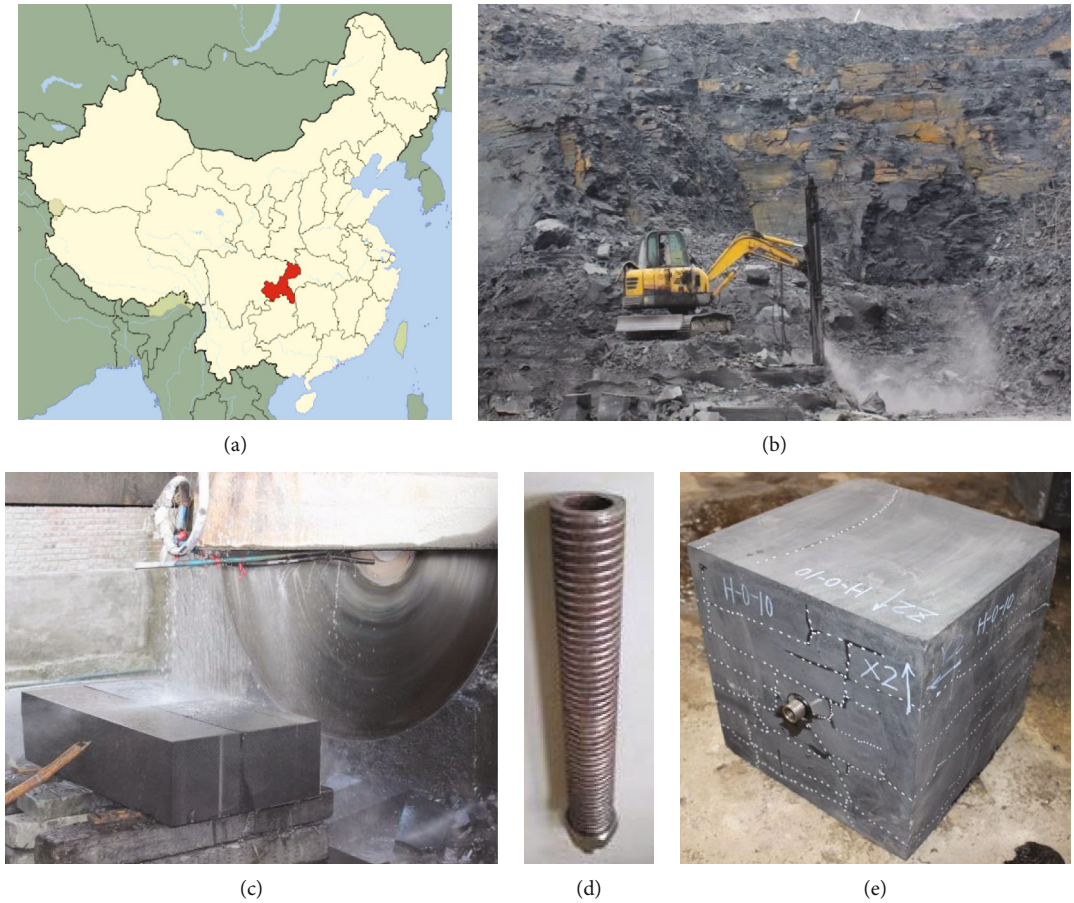

Figure 1: Preparation of shale samples for refracturing test. (a) The location of the shale outcrop; (b) removing the weathered surfaces of the broken shale blocks; (c) large samples are cut into 300 mm × 300 mm × 300 mm cubic samples; (d) simulated casing; (e) prepared standard fracturing samples.

mineralogical compositions of shale samples are 1.74% kaolinite, 1.42% Montmo rillonite, 3.15% illite, 58.70% quartz, 2.81% Cristobalit, 12.64% Albite, 5.59% calcite, 5.85% Muscovite, 4.23% Pyrite, and 3.87% Ankerite. The average density is 2.665 g/cm^3 with around 1.24% porosity. Some physical properties and mechanical properties in triaxial fracturing test are listed in Table 1.

After removing the weathered surfaces of irregular shale blocks, excavators were used to collect large shale samples. Then, a large cutting machine is used to process the shale sample into a cube sample of 300 mm × 300 mm × 300 mm. The horizontal well was simulated by drilling a hole with a depth of 165 mm to ensure an open hole section (depth of 30 mm) in the middle of the cubes; the axis of the borehole is parallel to the bedding plane, as shown in Figure 1(e). High-strength epoxy glue was used to seal the casing and wellbore annular space. A 30 mm long hole without casing was used as the fracture section.

Table 1: Material parameters of shale rock in true triaxial fracturing tests.

Properties	Value
Young's modulus (GPa)	25.50
Uniaxial compressive strength (MPa)	109.10
Tensile strength (MPa)	9.50
Cohesive force (MPa)	20.35
Friction angle	36.12
Porosity (%)	1.24
Permeability (Darcy)	0.00004
Poisson's ratio	0.185
The average velocity (m/s)	4860

2.2. Experimental Facility. The hydraulic fracturing test system employed in this study consists of two parts: a true triaxial geotechnical engineering testing machine and hydraulic fracturing fluid servo pumping control system. Figure 2 is a technical route of real triaxial fracturing experimental system. Figure 3 shows the main components of the hydraulic fracturing system. Figure 3(a) is a true triaxial geotechnical engineering testing machine. The device has the function of true triaxial test. X (Left and right), Y (Vertical), and Z (Front and back) directions are independently pressurized by axial loading system, which can truly simulate the stress situation of underground rock strata. The maximum load in each direction can reach 3000 kN. The installation of fracturing

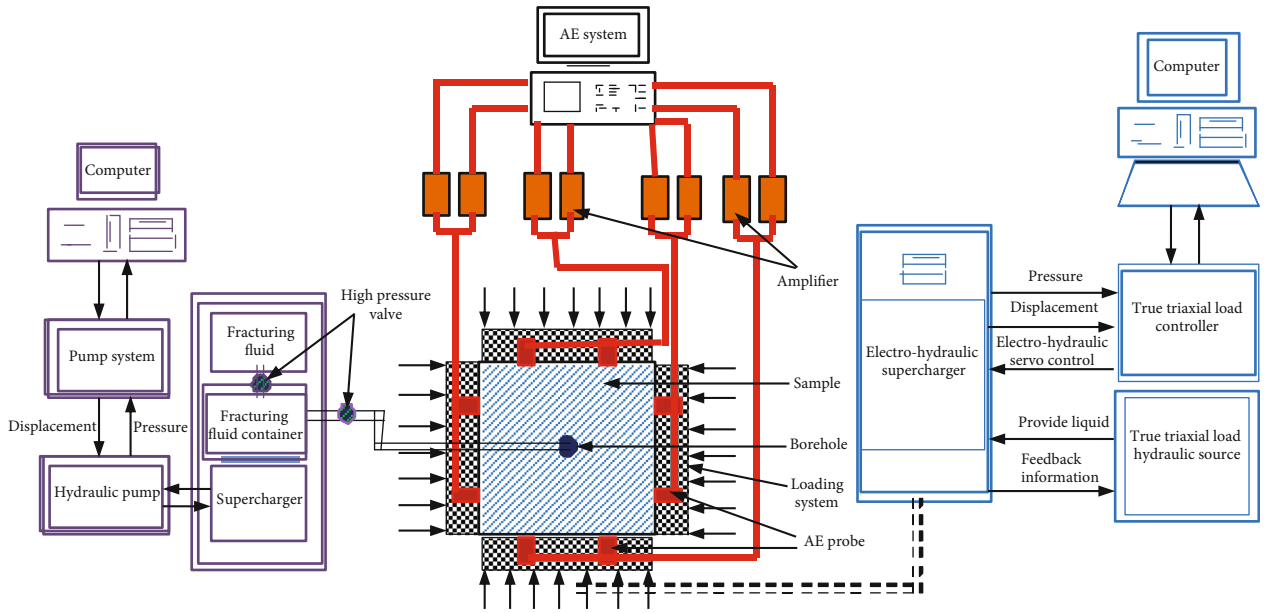

Figure 2: Technical route of real triaxial fracturing simulation experimental system.

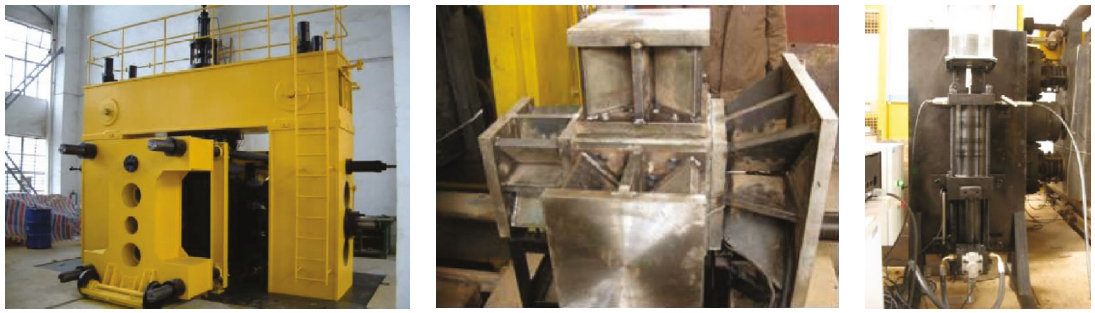

(a) (b) (c)

Figure 3: The main components of hydraulic fracturing system. (a) True triaxial loading frame. (b) Installation of fracturing specimen. (c) Servo control system.

specimens is shown in Figure 3(b). The loading can be applied synchronously in three directions according to the set proportion to ensure no damage to the sample before hydraulic fracturing.

The hydraulic fracturing pump servo control system is shown in Figure 3(c). The maximum load pressure is 100 MPa and the precision is at level 0.05 MPa. The effective volume of the supercharger is 800 mL, and the oil inlet and return inlet are equipped with accumulators to improve the dynamic response of the system and ensure the stability of the servo valve. The pump pressure is measured by the pressure sensor at the water inlet pipe. The rate of flow is measured indirectly by using highly precise electronic scale. The precision rate of flow control can reach 0.01 mL/s.

2.3. Experiment Procedures. It is difficult to carry out refracturing test in the laboratory, mainly because of how to effectively seal the fractures after initial fracturing. After a large number of laboratory tests, the test scheme of refracturing was determined.

First, the natural fractures and micro-open bedding planes of the processed **300 mm × 300 mm × 300 mm** cubes shale samples were marked. The sample was placed in the true triaxial loading chamber and subjected to three-dimensional in situ stresses. To avoid the unbalanced loading of triaxial stresses, three-dimensional in situ stresses were applied to the setting value with equal proportion loading. The schematic of the in situ stress loading direction used for hydraulic fracturing test is shown in Figure 4. The in situ stresses are set as follows: vertical stress is 19.30 MPa; the maximum horizontal stress is 21.00 MPa; and the minimum horizontal stress is 16.30 MPa. Then, the slickwater fracturing fluid was injected at the selected pump rate through the high-pressure pumping channel into the wellbore to induce fracturing fractures, and some water-soluble tracers were added into the slickwater fracturing fluid for a better observation of the fracturing fractures. The flow rate is 0.5 mL/s; when the fracturing pump pressure drops suddenly, it indicated that a new fracturing fracture appeared in the sample, continue pumping fracturing fluid, the pump pressure will not to rise or remain constant, and shut down the pumping

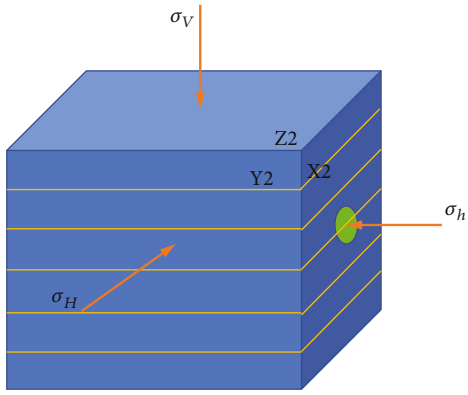

Figure 4: Schematic of the in situ stress loading direction for hydraulic fracturing.

system. The fracturing pressure was recorded automatically during the whole testing process.

The new fracturing fractures on the surface of the sample after initial fracturing were marked. If the tested sample has been performed with obvious macrofracture, the refracturing test is no longer performed, and the sample is opened for fracture description. If the tested sample is relatively complete, it is used to conduct a refracturing test. For the sample to be refractured, the plugging agent is injected into the wellbore, and a low pumping pressure is applied on the top of the plugging agent. The plugging agent is injected into the initial fracturing fracture by using the pressure difference. After the injection, the residual plugging agent at the bottom of the wellbore is removed and left for 2-3 days to fully solidify the plugging agent. Then, repeat the process of hydraulic fracturing test and another water-soluble tracer were added into the slickwater fracturing fluid for a better observation and distinction of the refracturing fractures. The characteristics of initial fracturing fractures and refracturing fractures were analyzed by cutting samples after refracturing test; the refracturing test parameters are listed in Table 2.

3. Experimental Results and Analysis

3.1. The Characteristics of Fracturing Pump Pressure Curve. The fracturing pump pressure is monitored during the whole testing process. The fracturing pump pressure is on the rise before the shale sample cracks, and it increases rapidly after an initial slow growth. When the sample cracks, the fracturing pump pressure drops to some extent.

Many researchers have carried out fracture morphological comparison under different fracturing parameters [4, 5]. However, there are differences in bedding plane and natural fractures of large-size samples. It is difficult to analyze the influence of fracturing parameters on fracturing fracture. In this study, under the condition of the same fracturing parameters, hydraulic fracturing test was carried out with shale samples from the same stratum. Figure 5 shows the fracturing pump pressure curve of shale samples; it can be seen that due to the difference in the internal structure of shale sample, the characteristics of fracturing pump pressure curve are different. In fracturing process, the fracturing pump pressure rose more steeply and went almost straight to the top; before the first breakdown pressure point, the fracturing pump pressure curves of different samples have similar characteristics.

In Figure 5(a), after an initial slow increase, the fracturing pump pressure increases rapidly, with only one peak point (31.09 MPa). When the fracturing breakdown pressure is reached, the fracturing pump pressure drops slightly. This indicates that the fracturing process occurs suddenly when the fracturing fluid pressure reached the fracturing breakdown pressure. The instantaneousness of the fracturing decided that the flow rate of fracturing fluid loss was much greater than fracturing fluid injection in the moment of fracture propagation, causing the fracturing pump pressure to drop rapidly. Then, the extension pressure was maintained above 22 MPa with slight fluctuations. After cutting of H-0-2 sample, the fracturing fracture characteristics indicate that the primary main hydraulic fracture encounters bedding surface, and it turns and extends, forming the bedding fracture with certain degree of fluctuation. It shows that the fracture propagation needs to overcome applied stress. In Figure 5(b), the highest fracturing pump pressure (32.01 MPa) appeared in the initial fracturing breakdown pressure; then, the fracturing pump pressure falls to 5.79 MPa rapidly. With the continuous injection of fracturing fluid, the fracturing pump pressure keeps increasing, but it is lower than the initial fracturing breakdown pressure, and multiple fracturing breakdown points were formed. The results indicate that the specimen has undergone several initiations of local fracturing fractures. In the comprehensive analysis of fracturing fracture morphology of H-0-7samples, the main hydraulic fractures communicate with several bedding fractures, forming a complex fracture network during the process of fracturing fracture propagation, In Figure 5(c), the highest fracturing pump pressure (32.93 MPa) appeared in the second fracturing breakdown pressure, corresponding to the fracturing rupture processes, the fracturing pump pressure falls rapidly to 13.70 MPa. After the second rupture, the fracturing pump pressure increased slightly with the injection of fracturing fluid, then the fracturing pump pressure is stable between 18.85 MPa and 19.60 MPa, and the fracturing fracture continue to expand. This phenomenon shows that a stable fracturing fracture channel has been formed in the sample, and the fracturing fluid has stable seepage after overcoming the in situ stress and fracture friction. In Figure 5(d), the fracturing breakdown pressure is highest among the four samples. It contains one main fracturing breakdown pressure with multiple low fracturing breakdown pressure points. The maximum fracturing breakdown pressure is twice that of low fracturing breakdown pressure. This indicates that fracturing fractures of different scales have been formed during the fracturing process.

3.2. Impacts of Bedding Plane or Natural Fracture on Fracture Propagation. The activation of pre-existing natural fracture or bedding plane is the optimum conditions for the formation of complex fractures. To investigate the interactions of pre-existing natural fracture or bedding plane and fracturing fractures, the samples were opened to compare and described the fracturing fractures after hydraulic fracturing test. Although the samples used in the study were from the same formation, affected by pre-existing natural fracture or

Table 2: The summary of refracturing test parameters.

Sample number	Three-dimensional in situ stress. (MPa)			$(\sigma_H - \sigma_h)/\sigma_h$	Flow rate (mL/s)	Initial fracturing breakdown pressure (MPa)	Refracturing breakdown pressure (MPa)
	σ_v	σ_H	σ_h				
H-0-2	19.3	21.0	16.3	0.29	0.5	31.09	/
H-0-7	19.3	21.0	16.3	0.29	0.5	32.01	/
H-0-15	19.3	21.0	16.3	0.29	0.5	31.74	/
H-0-19	19.3	21.0	16.3	0.29	0.5	37.35	/
H-0-4	19.3	21.0	16.3	0.29	0.5	30.90	27.93
H-0-6	19.3	21.0	16.3	0.29	0.5	29.49	38.65
H-0-10	19.3	21.0	16.3	0.29	0.5	29.77	35.29

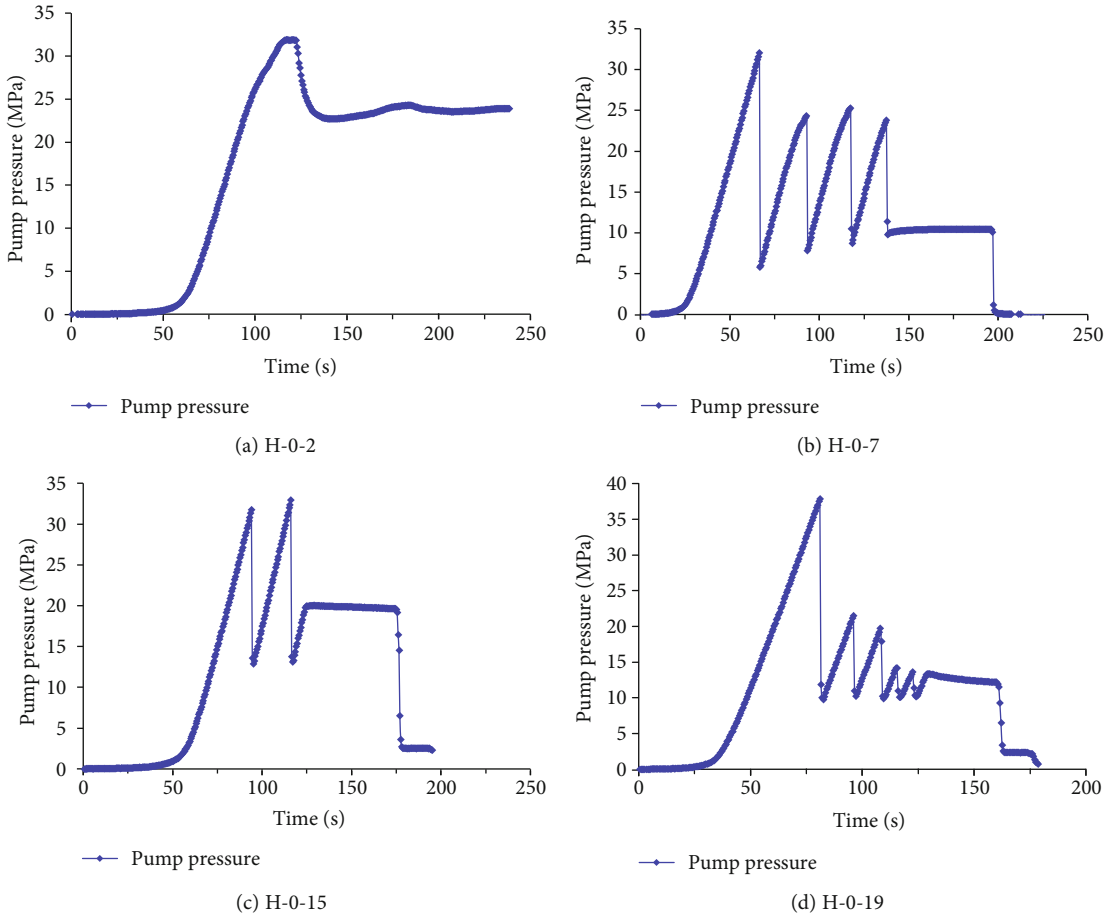

Figure 5: The injection fracturing pressure curve of shale samples.

bedding plane, under the same test parameters, the fracture morphology characteristics is different. The fracture morphology of the four samples after initial fracturing is shown in Figure 6. These four groups of samples have formed macrofracture after initial fracturing, which cannot be used to carry out refracturing test.

After hydraulic fracturing, the shale samples were opened along the hydraulic fractures and opened bedding surface by geological hammering, and the fracture morphology were observed and recorded. Different modes of fracture initiation and propagation can be seen in Figure 6. Most of the fracturing fractures were initiated from the open hole section to form a transverse main fracturing fracture that is perpendicular to the minimum horizontal principal stress. In Figure 6(a), when the main fracturing fracture expands to the weak bedding plane, the main fracturing fracture does not continue to expand, but turns to the direction of bedding plane to initiation and propagation. Affected by shale anisotropy, the fracture surface shows fluctuation. Because of the tensile failure is the main failure in fracturing test, corresponding to Figure 5(a), the extension pressure of uneven bedding surface is relatively high, and the fracturing

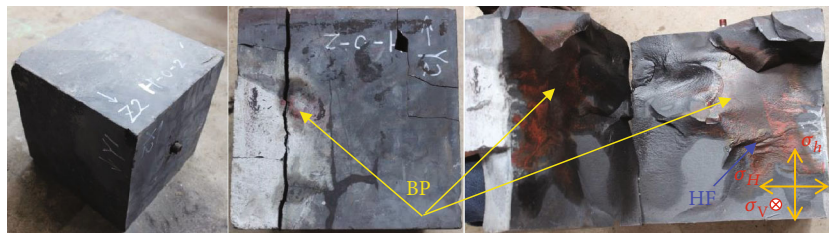

(a) H-0-2

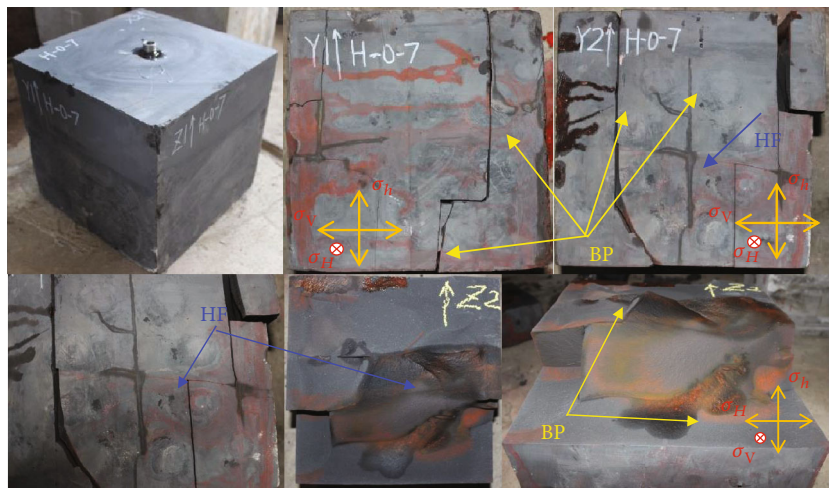

(b) H-0-7

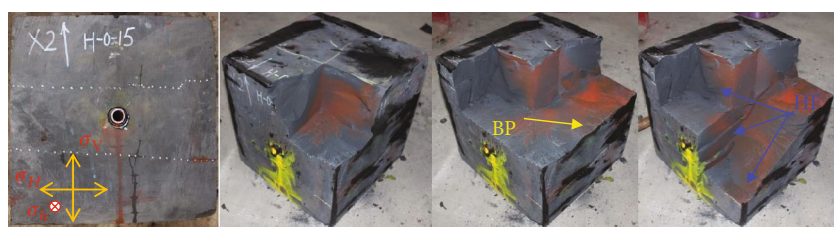

(c) H-0-15

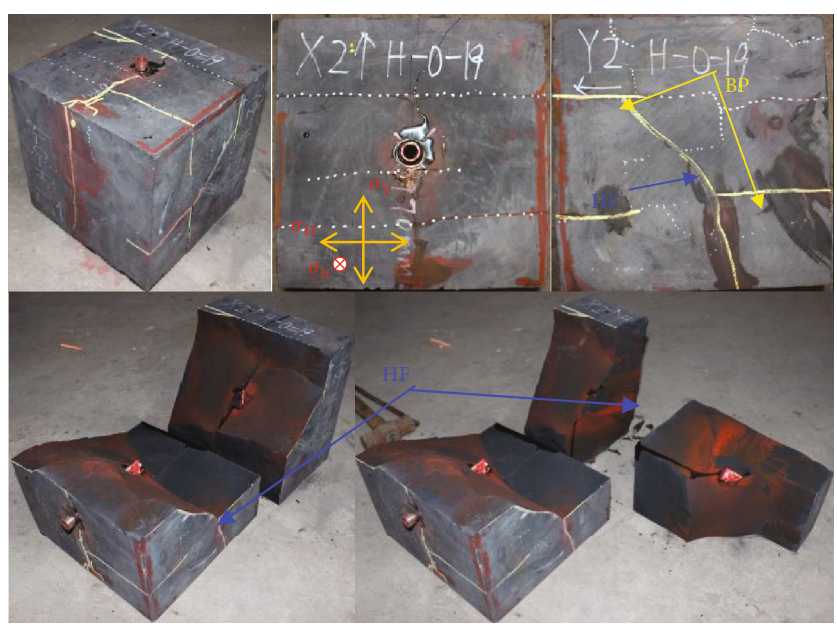

(d) H-0-19

Figure 6: The fracture propagations of the samples after initial fracturing. BP: bedding plane; HF: hydraulic fracture.

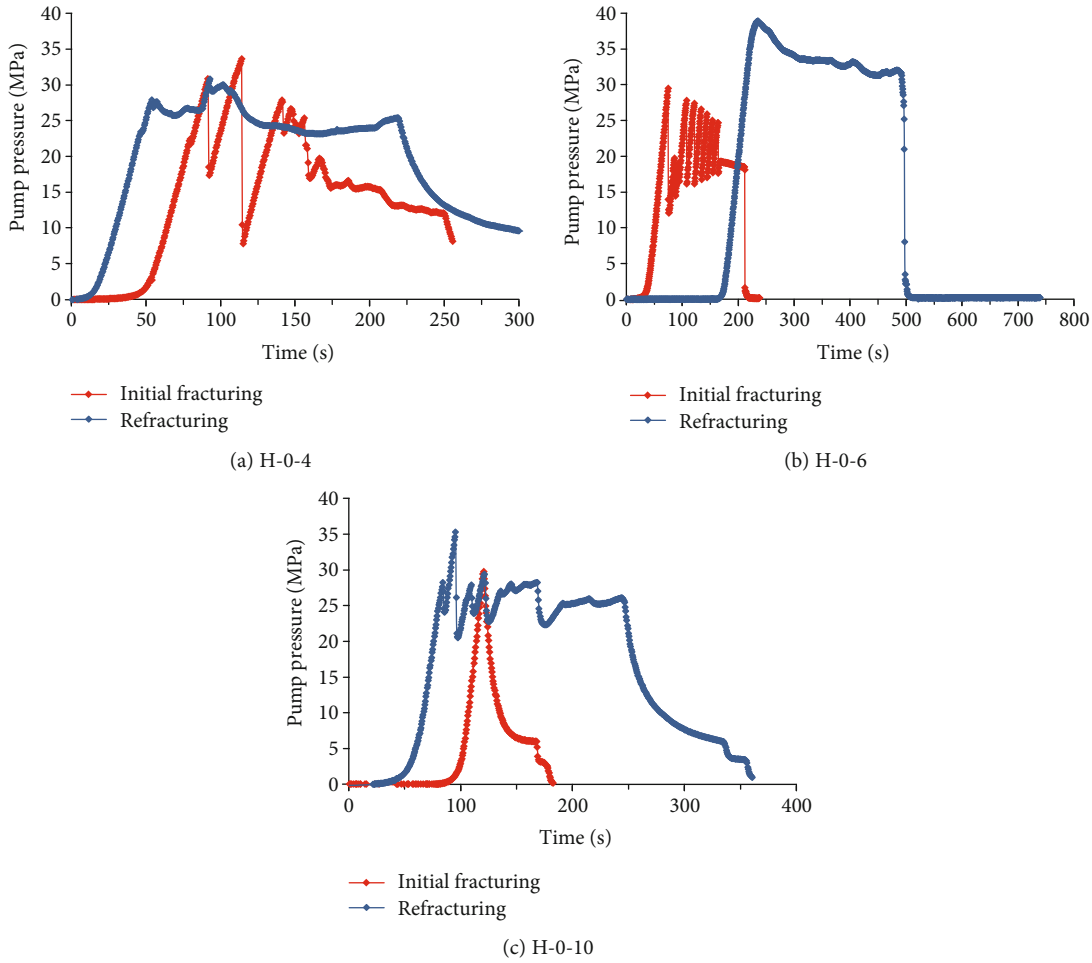

Figure 7: Characteristics of the refracturing pump pressure curve.

fracture complexity is relatively low after hydraulic fracturing. In Figure 6(b), it can be seen from the description of the external surface and opened fracturing fracture surface that the complexity of fracture formed of H-0-7 is higher than that of the other samples. The main hydraulic fracturing communicates multiple bedding planes, in both horizontal and vertical directions; the fracture after hydraulic fracturing is more consistent with the description of "complex fracture network" than simple fracture. In Figures 6(c) and 6(d), a main hydraulic fracturing fracture is created along the direction of maximum horizontal stress, then deviates when the main fracturing fracture extension encountered the pre-existing natural fractures, and the approximately crisscross fracture plane is formed. Through fracture morphology analysis after hydraulic fracturing, the fracturing pump pressure curves are found to be consistent with fracture propagation patterns. When the fracturing pump pressure occurred multiple fracturing fluctuation points, the fracture morphology formed after fracturing is more complex; when the fracturing pump pressure has only one or two fracturing fluctuation points, simple fracture characteristics are formed.

3.3. The Characteristics of Refracturing Pump Pressure Curve. After hydraulic initial fracturing, shale samples with fracturing fractures but without macrofracture surfaces were selected for refracturing test. Three samples with different initial fracturing pump pressure characteristics were carried out for refracturing tests. The refracturing pump pressure curve is shown in Figure 7. Through the refracturing pump pressure curve, it can be found that the characteristics of fracturing pump pressure after initial fracturing affect the characteristics of refracturing pump pressure curve. When the initial fracturing pump pressure curve has been occurred multiple fracture points, the refracturing pump pressure curve only has one fracturing breakdown pressure point, while when the initial fracturing pump pressure curve has only one fracturing breakdown pressure point, multiple fracturing fluctuation points appear in the refracturing process. This indicates that the characteristics of pump pressure curve can be used as an index to evaluate the effect of primary fracturing and whether it is necessary to carry out refracturing.

In Figure 7(a), the highest fracturing pump pressure after initial fracturing is not at the first breakdown pressure. After the initial fracturing fracture is temporarily blocked, refracturing test is carried out. The fracturing pump pressure rises more sharply and went almost straight to the breakdown pressure point, then the fracturing pump pressure drops slightly, and the second breakdown pressure point is reached after the fracturing fluid continues to be pumped. Then, the refracturing pump pressure keeps at a high value for a long

time and enters the stage of fracture expansion. There are only two pressure fluctuations in the sample during refracturing. This indicates that the fracture morphology produced during refracturing is relatively simple.

As can be seen in Figure 7(b), there are multiple peak points of the initial fracturing pump pressure; the characteristics of fracturing pump pressure curve is similar to H-0-7 sample after initial fracturing. According to the preliminary analysis of the fracturing fracture surface and fracturing pump pressure curve, the relatively complex fractures have been formed after initial fracturing. When the initial fracturing channel is temporarily blocked, the fracture initiation pressure of refracturing is higher than the maximum fracturing pump pressure of the initial fracturing, and only one breakdown pressure point occurred. The maximum fracturing pump pressure for refracturing reached to 38.65 MPa. After that, the refracturing pump pressure is maintained at a high level in extended fracturing; when the fracturing fluid expands to the sample boundary, the refracturing pump pressure drops rapidly. In Figure 7(c), during the initial fracturing process, the fracturing pump pressure is 29.77 MPa, and then falls rapidly. The characteristic of fracturing pump pressure curve is simple. This indicates that the sample has formed a fracturing fluid channel after initial fracturing. Moreover, the fracturing morphology formed may be relatively simple. In the process of refracturing, the fracturing pump pressure quickly reached to 27.61 MPa, and after a small drop, it rose again to 35.29 MPa, higher than the initial fracturing breakdown pressure. Then, the refracturing pump pressure curve remained fluctuating at a relatively high level (16~20 MPa). When the servo hydraulic fracturing pump was turned off, the fracturing curve dropped rapidly. Both the fracturing pressure and the overall pressure of the refracturing are higher than that of the initial fracturing; on the one hand, it shows that the initial fracturing fracture has been effectively sealed; on the other hand, it indicates that the sample has produced new hydraulic fractures. The violent fluctuation of refracturing pump pressure indicates that there are multiple initiations and extension of fracturing fractures and the fracturing fractures may become more complex.

3.4. The Interference Characteristics of Refracturing and Initial Fracturing Fractures. Morphological characteristics of refracturing fractures after opened the samples are shown in Figure 8. After the initial fracturing fractures are temporarily blocked, the fracture morphology formed by refracturing is shown in Figure 8(a). As can be seen from Figure 8(a), the tracer on fracturing fracture surface is observed; comparative analysis of the tracer characteristics, after initial hydraulic fracturing, a complex fracture network with a main fracturing fracture perpendicular to the horizontal minimum principal stress, is formed and a single natural fracture surface is approximately along the bedding plane, perpendicular to the vertical stress. Due to the same in situ stress conditions, after refracturing, an almost parallel refracturing fracture is formed the initial fracturing fracture. Disturbed by the initial fracturing fracture, the propagation path of the refracturing fracture is deviated. Meanwhile, some weak bedding surfaces are opened during the refracturing process. During refracturing fracture propagation, the initial fracturing fracture was communicated after bypassing the temporary plugging point. In the case of continuous fracturing fluid pumping, the fracture extends to the sample boundary. The refracturing result of sample H-0-4 shows that, when relatively complex fracturing fractures have been formed in the initial fracturing, the refracturing test can open the range of the unreconstructed zone effectively.

In Figure 8(b), it was shown that a complex fracturing fracture network with a large volume of fracture reconstruction includes one main fracturing fracture and four activated weak bedding planes, and the main fracturing fracture communicates multiple bedding planes. According to H-0-6 fracturing sample after opened and analysis of the fracturing pump pressure curve characteristics, it indicates that complex fracture networks have been formed during initial fracturing; the fracturing fluid containing the red tracer occupied most of the fracturing fractures. This indicates that corresponding to the fluctuation of fracturing pump pressure, the main fracturing fracture opens multiple bedding planes during the expansion, and the sample has been fully transformed after initial fracturing. For shale samples with multiple temporarily blocked fracturing fractures, when refracturing is carried out under the same three-direction in situ stress, the propagation path of refracturing fracture will be affected by the initial fracturing fracture, and the initiation and expansion directions may be changed. After refracturing sample H-0-6, new main fracturing fractures are formed near the initial main fracturing fracture, and the main refracturing fracture was along the direction of the horizontal minimum stress and intersects with the initial fracturing fracture. It can be observed from the fracturing fracture trace that the fracturing fluid containing yellow tracer and red tracer is mixed; this means that after bypassing the temporary plugging point, the new refracturing fracture turns to the initial fracturing fracture and continues to expand. The results of refracturing showed that the refracturing effect is not obvious for the samples after sufficient modification.

In Figure 8(c), after initial fracturing, a slightly inclined hydraulic fracturing fracture was formed in the middle of the sample. The fracture is slightly extended in several adjacent bedding planes, and the fracture distribution is approximately perpendicular to horizontal minimum principal stress. It is preliminarily speculated that this is a main fracturing fracture surface, with the initiation position at the bottom of the wellbore in the open hole section. After refracturing, there is another yellow tracer overflow at the main fracturing fracture; it indicates that there may be a new fracturing fracture initiation and propagation along this direction. Meanwhile, new fracturing fractures containing yellow tracer were found in multiple locations of the whole plane. Most of the fractures were distributed along the bedding plane, and there were also a few vertically distributed fracturing fractures, which communicated the adjacent bedding planes. When the upper left part of the sample was cut open, large amounts of red and yellow tracer residues were observed in the bedding surface, indicating that the bedding plane was opened during the initial fracturing and continued to expand during the refracturing process. Three parallel and

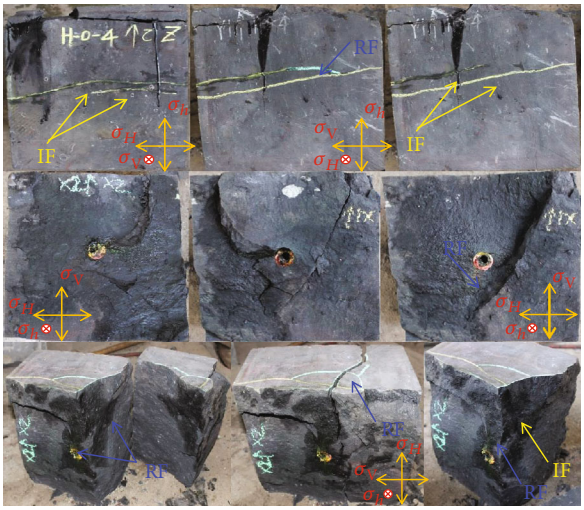

(a) H-0-4 (IF: initial fracturing fractures; RF: refracturing fractures)

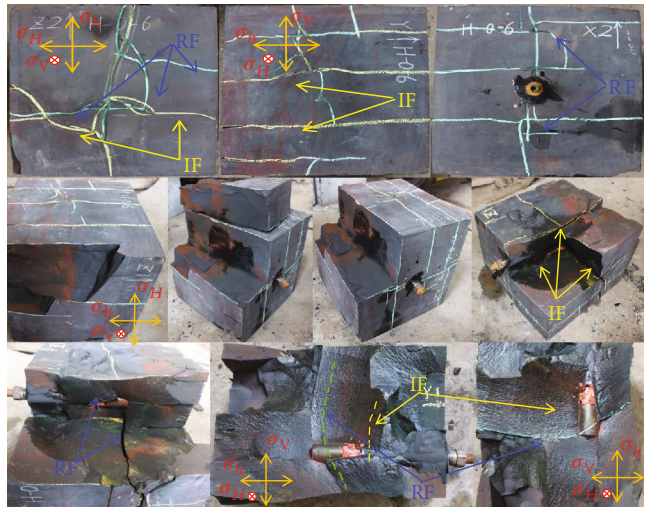

(b) H-0-6 (IF: initial fracturing fractures; RF: refracturing fractures)

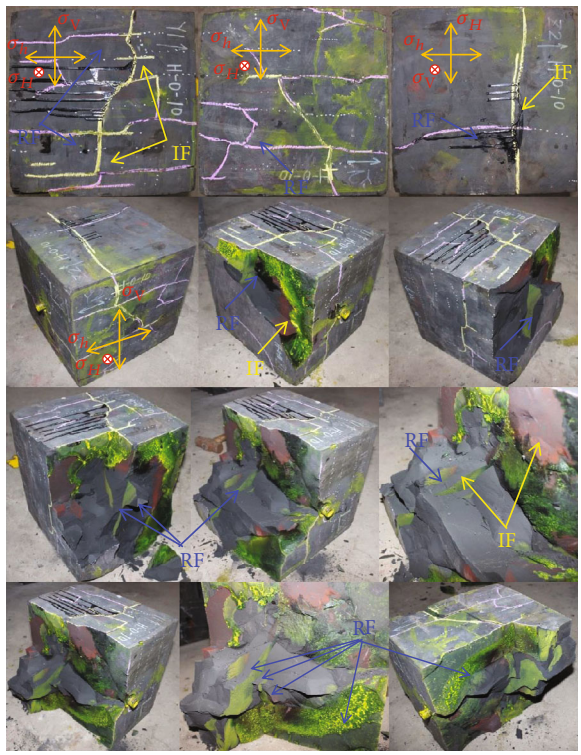

(c) H-0-10 (IF: initial fracturing fractures; RF: refracturing fractures)

Figure 8: Morphological characteristics of refracturing fractures. BP: bedding plane; 392 HF: hydraulic fracture. The red tracer is initial fracturing; the yellow tracer is 393 refracturing.

closely adjacent transverse fractures were found. The fracturing fracture was roughly perpendicular to horizontal minimum principal stress, and the fracturing fracture initiation was in the open hole section. One of the fracturing fractures has a red tracer inside and a yellow tracer outside, indicating that the fracture was formed during the initial fracturing and expanded during the refracturing process. The other two fracturing fractures both with yellow tracer were newly formed during the refracturing process. Base on comprehensive observation and analysis, it can be seen that the main fracturing fracture of a vertical wellbore is formed after initial fracturing, but the extent of fracturing fracture and the opening degree of the bedding surface are inadequate modification, and the reconstruction is insufficient. During the refracturing process, two new transverse main fracturing fractures were formed, and the original transverse main fracturing fracture continued to expand. Therefore, the bedding planes were fully opened, forming a crisscrossing fracture with multiple transverse fractures and bedding planes and the improvement effect was relatively ideal. According to the results of the experimental study, for the formation with simple fracturing fracture formed after initial fracturing,

refracturing can be adopted to increase the fracture complexity of formation through temporary plugging.

3.5. Stress Field Analysis around Initial Fracturing Fracture. Shale gas reservoirs are extremely low in porosity and permeability; horizontal well staged fracturing is used to communicate natural fractures and weak bedding planes. With the technology of segmental fracturing in horizontal wells, the generation of multiple fractures is in sequence. When the initial fracturing crack is formed, it will affect the stress distribution in a certain range around the initial fracturing crack. The induced stress field is generated around the fracture, and the induced stress field will have a certain influence on the initiation and extension of the follow-up fracturing fracture. At present, the calculation of induced stress field mainly depends on the analytical formula of classical fracture mechanics theory [20].

According to the fracture mechanics theory, a two-dimensional-induced stress field calculation model is established based on the assumption of homogeneity, isotropy, and plane strain; the calculation schematic diagram of fracturing fracture induced stress field as shown in Figure 9.

It is assumed that the fracturing fracture is vertical, the longitudinal section is elliptical, the height is H, and Z-axis is along the fracture height direction. X-axis is along the horizontal well bore and Y-axis is along the direction of the maximum horizontal stress. It is assumed that the tensile stress is positive and the comprehensive stress is negative. The induced stress at any point (X, Y, and Z) is as follows [21]:

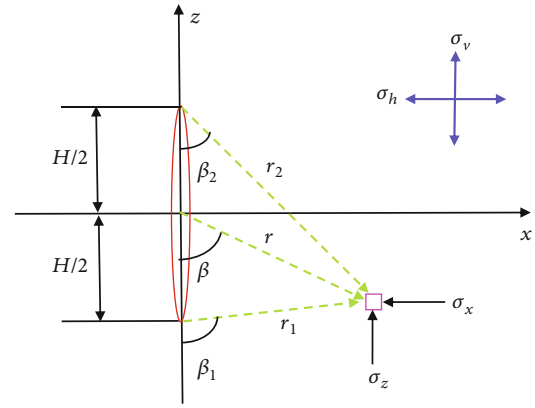

Figure 9: Schematic diagram of fracturing fracture induced stress field.

$$\begin{cases} \sigma_x = -p\dfrac{r}{c}\left(\dfrac{c^2}{r_1 r_2}\right)^{3/2} \sin\theta \sin\left[\dfrac{3}{2}(\theta_1+\theta_2)\right] + p\left[\dfrac{r}{(r_1 r_2)^{1/2}} \cos\left(\theta - \dfrac{1}{2}\theta_1 - \dfrac{1}{2}\theta_2\right) - 1\right], \\ \sigma_z = p\dfrac{r}{c}\left(\dfrac{c^2}{r_1 r_2}\right)^{3/2} \sin\theta \sin\left[\dfrac{3}{2}(\theta_1+\theta_2)\right] + p\left[\dfrac{r}{(r_1 r_2)^{1/2}} \cos\left(\theta - \dfrac{1}{2}\theta_1 - \dfrac{1}{2}\theta_2\right) - 1\right], \\ \sigma_y = \nu(\sigma_x + \sigma_z), \\ \tau_{xz} = -p\dfrac{r}{c}\left(\dfrac{c^2}{r_1 r_2}\right)^{3/2} \sin\theta \sin\left[\dfrac{3}{2}(\theta_1+\theta_2)\right], \end{cases} \tag{1}$$

where $c = H/2$, σ_x, σ_y, and σ_z are the induced three normal stress components (MPa); τ_{xz} is the shear component (MPa); p is the fluid pressure (MPa); ν is the Poisson ratio. The relationship of the parameters is as follows:

$$\begin{cases} r = \sqrt{x^2 + z^2}, \\ r_1 = \sqrt{x^2 + (c-z)^2}, \\ r_2 = \sqrt{x^2 + (c+z)^2}, \\ \theta = \arctan\left(-\dfrac{x}{c}\right), \\ \theta_1 = \arctan\left(\dfrac{x}{c-z}\right), \\ \theta_2 = \arctan\left(-\dfrac{x}{c+z}\right). \end{cases} \tag{2}$$

In situ stress is determined by σ_x, σ_y, and σ_z. The stress field around the later crack should be the sum of the induced stress of the initial fractures and ground stress of the previous crack. According to the principle of superposition, the stress field around the nth fracture is [22, 23].

$$\begin{cases} \sigma'_{H(n)} = \sigma_H + \nu\left(\sum_{i=1}^{n-1}\sigma_{x(in)} + \sum_{i=1}^{n-1}\sigma_{z(in)}\right), \\ \sigma'_{h(n)} = \sigma_h + \sum_{i=1}^{n-1}\sigma_{x(in)}, \\ \sigma'_{v(n)} = \sigma_v + \sum_{i=1}^{n-1}\sigma_{z(in)}. \end{cases} \tag{3}$$

$\sigma'_{H(n)}$, $\sigma'_{h(n)}$, and $\sigma'_{v(n)}$ are the three principal stresses around the nth fracture, MPa; $\sigma_{x(in)}$, $\sigma_{y(in)}$, and $\sigma_{z(in)}$

are the induced stress components around the nth fracture caused by the *i*th fracture, MPa.

When a new fracture is formed, it produces an induced stress field which can be calculated by formula (1). Superimpose this new induced stress field into the old one and so on; the final stress field can be obtained from equation (3). This method only considers the effect of hydraulic fracture on stress field and ignores the effect of horizontal well. So, it is limited and cannot provide the exact value of the stress field. Because the stress field around the horizontal wellbore of shale reservoir changes dramatically, the effect of horizontal wellbore on stress field distribution should be consider. The induced stress field is mainly affected by the internal pressure, fracture length, and fracture spacing. It is necessary to study the effect of initial fracturing fracture on postfracture during refracturing by laboratory test. The obtained fracture characteristics can be used to analyze the fracturing fracture interference. As can be seen in Figure 8, the initial fracturing fracture has some interference to the refracturing fracture, which leads to the deviation of the propagation path of refracturing fracture.

4. Discussion

Refracturing can open new flow channels in oil and gas reservoirs and communicate with the unused reservoir of the old fracture to increase oil and gas production. The refracturing treatment design for shale gas wells is largely based on the original wellbore completion and reservoir characteristics, rock mechanics, geostress characteristics, and fracture geometry [10]. During the initial hydraulic fracturing, the fracture morphology formed is of great significance to the subsequent refracturing. At present, there are few methods to identify and evaluate the fracturing fracture. In this paper, the indoor hydraulic fracturing test is used to obtain the morphological characteristics of refracturing under different initial fracture characteristics, which is of certain significance to study the fracturing timing and location selection of refracturing wells. The direction of fracture initiation and extension depends on the in situ stress state. The in situ stress difference at different locations varies with time, and the initial far-field stress difference is an important condition to determine whether a new fracture is generated or not [24]. The induced stress generated by the initial fracturing fracture can be preliminarily evaluated by combining the analytical method with hydraulic fracturing test. The results showed that for reservoir with simple initial fracturing fractures, the complexity fracturing fracture can be increased by refracturing after temporary plugging. The effect of refracturing is not obvious for the reservoir with complex initial fracturing fractures. Due to the influence of shale bedding and natural fracture, fracture morphology obtained after hydraulic fracturing may be quite different in the same shale reservoir. Therefore, comprehensive evaluation such as pumping pressure, initial gas production, and profile test is needed to evaluate whether refracturing is necessary. The results can be used to evaluate the timing and location of refracturing in shale reservoirs.

5. Conclusions

A series of large-scale true triaxial hydraulic fracturing and refracturing tests were conducted on cube shale samples. The fracturing fracture expansion behavior after refracturing was studied and some suggestions on whether refracturing was required after initial fracturing were given. The following conclusions can be drawn:

(1) The characteristics of bedding plane and natural fracture development in shale samples directly affect the effect of hydraulic fracturing reconstruction. The fracturing pump pressure curve and fracture morphology with the same batch of shale samples are significantly different under the same fracturing parameters

(2) The characteristics of fracturing pump pressure curve indicated the evolution of hydraulic fractures, including initiation and propagation of hydraulic fracturing and communication of multiple fractures. The violent fluctuation of the fracturing pump pressure curve reflects the repeated fracture characteristics

(3) The fracturing breakdown pressure of refracturing is generally slightly higher than that of the initial fracturing breakdown pressure. Under the influence of stress induced by the initial fracturing fracture, the propagation path of the refracturing fracture is deviated

(4) Before refracturing test, it is necessary to analyze the fracturing pump pressure curve characteristics of the initial fracturing. In the case of a formation that has been sufficiently fractured after initial fracturing, there are almost new fractures after refracturing. Therefore, there is no need for refracturing

(5) In the formation with simple fracture after initial fracturing, it is necessary to block temporarily initial fracturing fracture before refracturing

In this study, an effective method of refracturing test in laboratory was established. The effect of refracturing with different initial fracturing fracture morphology was analyzed. In the refracturing test, the initial fracturing and refracturing have the same in situ stress. However, in the actual fracturing construction process, as the induced stress around fractures are caused by the initial fracturing fractures, the three in situ stress parameters should be superposition. Further relevant studies will be carried out in the future.

Data Availability

The data used to support the findings of this study are available from the corresponding author upon request.

Conflicts of Interest

The authors declare that there are no conflicts of interest regarding the publication of paper.

Authors' Contributions

Y.G. and L.W. conceived and designed the experiments; J.X. and X.C. processed and analyzed the experimental data; Y.H. and J.Z. performed the experiments; X.Z. provided the experimental support. All authors have read and approved the final manuscript.

Acknowledgments

The research was supported by the National Natural Science Foundation of China (51574218), National Science and Technology Major Project of China (2017ZX05005-004, 2017ZX05036-003), and Research on Key Scientific and China Postdoctoral Science Foundation (2019M662918) and Technical Issues in Exploration and Development of Shale Gas (XDB10040200), CAS pilot project (B). We would like to express our greatest gratitude for their generous support.

References

[1] M. C. Vincent, "The next opportunity to improve hydraulic-fracture stimulation," *Journal of Petroleum Technology*, vol. 64, no. 3, pp. 118–127, 2012.

[2] Y. P. Da, W. Zhao, and X. Q. Bo, "Study on fracture pattern law for re-fracturing in low permeability reservoir," *Fault-Block Oil & Gas Field*, vol. 19, no. 6, pp. 781–784, 2012.

[3] B. Hou, R. Zhang, Y. Zeng, W. Fu, Y. Muhadasi, and M. Chen, "Analysis of hydraulic fracture initiation and propagation in deep shale formation with high horizontal stress difference," *Journal of Petroleum Science and Engineering*, vol. 170, pp. 231–243, 2018.

[4] P. Hou, F. Gao, Y. Ju et al., "Experimental investigation on the failure and acoustic emission characteristics of shale, sandstone and coal under gas fracturing," *Journal of Natural Gas Science and Engineering*, vol. 35, pp. 211–223, 2016.

[5] P. Tan, Y. Jin, K. Han et al., "Analysis of hydraulic fracture initiation and vertical propagation behavior in laminated shale formation," *Fuel*, vol. 206, pp. 482–493, 2017.

[6] J. Zhou, Y. Jin, and M. Chen, "Experimental investigation of hydraulic fracturing in random naturally fractured blocks," *Int J Rock Mech Min Sci*, vol. 47, no. 7, pp. 1193–1199, 2010.

[7] X. Chang, Y. Guo, J. Zhou, X. Song, and C. Yang, "Numerical and experimental investigations of the interactions between hydraulic and natural fractures in shale formations," *Energies*, vol. 11, no. 10, p. 2541, 2018.

[8] Y. Zhang, J. He, X. Li, and C. Lin, "Experimental study on the supercritical CO_2 fracturing of shale considering anisotropic effects," *Journal of Petroleum Science and Engineering*, vol. 173, no. 173, pp. 932–940, 2019.

[9] S. M. Patel, C. H. Sondergeld, and C. S. Rai, "Laboratory studies of hydraulic fracturing by cyclic injection," *International Journal of Rock Mechanics and Mining Sciences*, vol. 95, pp. 8–15, 2017.

[10] M. Shah, S. Shah, and A. Sircar, "A comprehensive overview on recent developments in refracturing technique for shale gas reservoirs," *Journal of Natural Gas Science and Engineering*, vol. 46, pp. 350–364, 2017.

[11] S. S. Yi and M. M. Sharma, "A new method to calculate slurry distribution among multiple fractures during fracturing and refracturing," *Journal of Petroleum Science and Engineering*, vol. 170, pp. 304–314, 2018.

[12] J. S. Curnow and A. N. Tutuncu, "A coupled geomechanics and fluid flow modeling study for hydraulic fracture design and production optimization in an Eagle Ford shale oil reservoir," in *SPE Hydraulic Fracturing Technology Conference*, Woodland, Texas, USA, February 2016.

[13] C. L. Fitzpatrick and T. Williams, "Seismic-to-simulation for unconventional reservoir development," in *SPE Reservoir Characterisation and Simulation Conference and Exhibition*, Abu Dhabi, UAE, October 2011.

[14] B. Teng and H. A. Li, "A semi-analytical model for characterizing transient flow behavior of reoriented refractures," *Journal of Petroleum Science and Engineering*, vol. 177, pp. 921–940, 2019.

[15] M. A. Aghighi and S. S. Rahman, "Horizontal permeability anisotropy: effect upon the evaluation and design of primary and secondary hydraulic fracture treatments in tight gas reservoirs," *Journal of Petroleum Science and Engineering*, vol. 74, no. 1-2, pp. 4–13, 2010.

[16] F. Zhang and M. Mack, "Integrating fully coupled geomechanical modeling with microsesmicity for the analysis of refracturing treatment," *Journal of Natural Gas Science and Engineering*, vol. 46, pp. 16–25, 2017.

[17] J. Guo, L. Tao, and F. Zeng, "Optimization of refracturing timing for horizontal wells in tight oil reservoirs: a case study of Cretaceous Qingshankou Formation, Songliao Basin, NE China," *Petroleum Exploration and Development*, vol. 46, no. 1, pp. 153–162, 2019.

[18] L. Shan, B. Guo, D. Weng, Z. Liu, and H. Chu, "Posteriori assessment of fracture propagation in refractured vertical oil wells by pressure transient analysis," *Journal of Petroleum Science and Engineering*, vol. 168, pp. 8–16, 2018.

[19] B. Wang, F. Zhou, D. Wang, T. Liang, L. Yuan, and J. Hu, "Numerical simulation on near-wellbore temporary plugging and diverting during refracturing using XFEM-Based CZM," *Journal of Natural Gas Science and Engineering*, vol. 55, pp. 368–381, 2018.

[20] Y. J. Zeng, C. H. Yang, and B. P. Zhang, *The theory and practice in shale gas development engineering*, Science press, 2017.

[21] I. D. Palmer, "Induced stresses due to propped hydraulic fracture in coalbed methane wells," in *Low Permeability Reservoirs Symposium*, Denver, Colorado, April 1993.

[22] X. Shang, S. He, and G. Liu, "Breakdown pressure calculation of staged fracturing for horizontal wells," *Oil Drilling & Production Technology*, vol. 31, no. 2, pp. 96–100, 2019.

[23] F. McNeil, K. A. W. Gijtenbeek, and M. V. Domelen, "New hydraulic fracturing process enables far-field diversion in unconventional reservoirs," in *SPE/EAGE European Unconventional Resources Conference and Exhibition*, Vienna, Austria, March, 2012.

[24] J. I. Elbel and M. G. Mack, "Refracturing: observations and theories," in *SPE paper 25464 presented at the 1993 SPE Production Operations Symposium*, Oklahoma City, March, 1993.